Pump-probe spectroscopy of two-body correlations in ultracold gases

Christiane P. Koch[1,*] and Ronnie Kosloff[2]

[1]*Institut für Theoretische Physik, Freie Universität Berlin, Arnimallee 14, 14195 Berlin, Germany*
[2]*Institute of Chemistry and The Fritz Haber Research Center, The Hebrew University, Jerusalem 91904, Israel*

(Dated: May 20, 2009)

We suggest pump-probe spectroscopy to study pair correlations that determine the many-body dynamics in weakly interacting, dilute ultracold gases. A suitably chosen, short laser pulse depletes the pair density locally, creating a 'hole' in the electronic ground state. The dynamics of this non-stationary pair density is monitored by a time-delayed probe pulse. The resulting transient signal allows to spectrally decompose the 'hole' and to map out the pair correlation functions.

PACS numbers: 03.75.Kk,32.80.Qk,82.53.Kp

Introduction Bose-Einstein condensation in dilute gases is determined by the nature of the two-body interactions between the atoms [1]. These microscopic interactions manifest themselves in two-body correlations and dictate the mesoscopic and macroscopic properties of the condensate. In the most simplified approach their effect is captured in a single parameter, the scattering length [1]. Measuring the scattering length corresponds to an indirect assessment of the pair correlations. A comprehensive study becomes possible if a timescales separation between the two-body interactions and the measurement can be generated. Here we suggest to employ pump-probe spectroscopy to unravel the dynamics of pair correlations in a many-body quantum system. The basic feasibility of such a combination of ultrafast and ultracold physics has been demonstrated in recent experiments on femtosecond photoassociation of ultracold rubidium atoms [2, 3].

Our scheme involves three short laser pulses and is sketched in Fig. 1 for the example of an ultracold gas of ^{87}Rb atoms. The pump pulse excites population from the electronic ground to an excited state, carving a 'hole' into the initial pair correlation function. The hole represents a non-stationary state that moves under the influence of the ground state Hamiltonian, cf. Fig. 1. A time-delayed probe pulse monitors the amount of probability amplitude in a range of internuclear distances. The largest probe signal is obtained when the probe detuning and spectral bandwidth are identical to the pump pulse. The dynamics are then monitored at the position where the hole was created. The probe windows are shown in orange in Fig. 1 (dotted for triplet, striped for singlet). Generally, the initial pair wave function of alkali atoms consists of a superposition of singlet and triplet components (only triplet wave functions are depicted in Fig. 1). Due to different effective C_3 coefficients in the excited state, the Condon radius for exciting the singlet and triplet components is not identical. This is reflected in different positions of the probe windows. Detection proceeds via the creation of molecular ions and is inspired by Refs. [2, 3]. Here, however, ground state amplitude is photoassociated and ionized simultaneously while in Refs. [2, 3] the ionization pulse by itself served as probe.

Pair correlations Formally, the dynamics of a many-body quantum system such as an ultracold gas at or near quantum degeneracy is described in terms of the Heisenberg equations of motion for the field operators that create or annhilate a particle at position $\vec{x}$. This approach is not feasible in general. A remedy is found by constructing effective mean-field theories [1]. For dilute gases where only two-body interactions are prominent, pair correlations constitute the leading order corrections to a single-

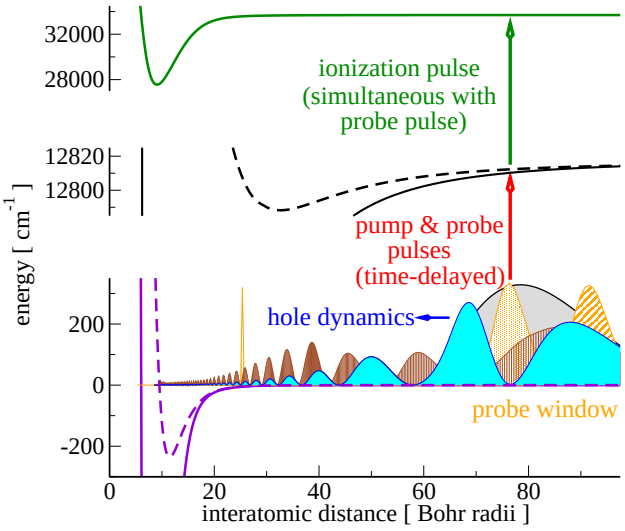

FIG. 1: (Color online) Pump-probe spectroscopy of dynamical two-body correlations: A pump pulse excites population from the electronic ground to the first excited state, leaving a hole in and transferring momentum to the ground state wave function. A time-delayed probe pulse monitors the amount of amplitude in the region where the hole was created. The potentials of the singlet ground state (lowest triplet state) and an exemplary excited state accessed from it are shown by solid (dashed) lines. For clarity only wavefunctions in the lowest triplet state are depicted – before the pulse (black line), at $t_{max} + 24$ ps, i.e. just after the pulse (blue filled) and at $t_{max} + 126$ ps (brown line). The probe windows are shown in orange (see text for details).

particle mean-field picture. For bosons, they can be incorporated explicitly by expanding the many-body wave function in cumulants [4] or correlation functions [5]. For dilute, weakly interacting Bose gases in a macroscopic trap, the extent of the pair correlations is much smaller than the condensate length scale and the pair dynamics are not affected by higher than second order terms. The pair correlation function, $\varphi(\vec{x},\vec{y};t) = \langle\hat{\psi}(\vec{x};t)\hat{\psi}(\vec{y};t)\rangle$ then simply satisfies the Schrödinger equation of two atoms colliding in free space [5]. The same holds for the first order cumulant [4].

We can therefore study pair correlation dynamics in a Bose-Einstein condensate by solving the time-dependent Schrödinger equation for a single low energy scattering state. The calculation requires a grid large enough to faithfully represent the scattering atoms. This is achieved by employing a mapped Fourier grid [6]. At higher temperatures, the bosonic nature of the atoms can be neglected. The ultracold thermal ensemble is then described by a Boltzmann average over all thermally populated two-body scattering states [7]. In particular, higher partial waves may then contribute to the pair correlation dynamics.

Model We consider two colliding ^{87}Rb atoms. Hyperfine interaction couples the ground state singlet and lowest triplet scattering channels. However, this interaction cannot be resolved on the timescales considered below. We therefore assume a superposition of singlet and triplet components, but neglect the effect of hyperfine interaction on binding energies and dynamics. The interaction of the atom pair with the pump pulse is treated within the dipole and rotating wave approximations [8]. Excitation is considered exemplarily into the $0_u^+(5s+5p_{3/2})$ and $0_g^-(5s+5p_{3/2})$ excited states. Details on the potentials are found in Ref. [8]. The time-dependent Schrödinger equation is solved using the Chebychev propagator. The collision energy of the initial pair correlations is chosen to correspond to $20\,\mu$K with 75% (25%) triplet (singlet) character. All wave functions are normalized to unity. Transform-limited Gaussian pulses with a full-width at half-maximum (FWHM) of 10 ps are used.

Characterization of the hole As sketched in Fig. 1, the pump pulse carves a hole into the ground state pair correlation function. The resulting non-stationary wave packet is a superposition of a few weakly bound vibrational wave functions and many scattering states [9]. The corresponding projections are shown in Fig. 2 for the triplet component of the 'hole', comparing two pump pulse detunings, $\Delta_L = \omega_L - \omega_{at}$, and three pump pulse energies, $\mathcal{E}_P$ (t_f denotes the time when the pump pulse is over). The detuning determines the Condon radius and hence the position, around which the hole is carved, $R_L \sim 76\,(48)\,a_0$ for $\Delta_L = -4.0\,(-14)\,\mathrm{cm}^{-1}$. This position is reflected in the weakly bound levels that are populated, predominantly the last bound level for $\Delta_L = -4.0\,\mathrm{cm}^{-1}$, and the second to last level for

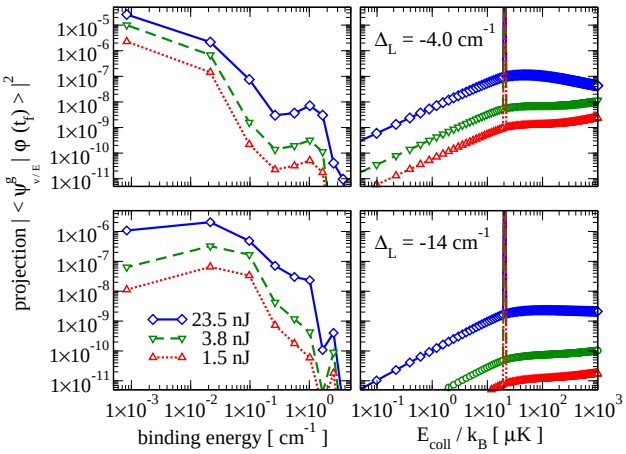

FIG. 2: (Color online) Characterizing the triplet component of the hole: Projection onto the bound levels (left) and onto the scattering states (right) for pump pulse detunings $\Delta_L = -4.0\,\mathrm{cm}^{-1}$ (upper panel) and $\Delta_L = -14\,\mathrm{cm}^{-1}$ (lower panel) and for three pump pulse energies.

$\Delta_L = -14\,\mathrm{cm}^{-1}$. The overall probability to populate weakly bound levels is larger for high pulse energy and small detunings. A pulse energy of 1.5 nJ is sufficient to deplete the population within the resonance window of the pump pulse (cf. the blue wave function in Fig. 1). At higher pulse energies, Rabi cycling within the resonance window sets in. It leads to larger populations in the bound levels but also to more redistribution among the scattering states.

Pump-probe spectra The dynamics of the non-stationary wave packet created by the pump pulse is monitored by a probe pulse that excites population to the first excited state. An ionization pulse is sent simultaneously with the probe pulse to transfer the excited state population to the Rb_2^+ ground state. That is, a two-color REMPI scheme is proposed such that the absorption of the probe pulse is translated into detection of molecular ions similar to Refs. [2, 3]. Assuming the probe pulse to be weak and the ionization step to be saturated, probe absorption can be modelled within first order perturbation theory [10]. The transient absorption signal is then represented by the time-dependent expectation value of a window operator, $\hat{\mathbf{W}}(\hat{\mathbf{R}}) = \pi(\tau_p E_{p,0})^2\,\mathrm{e}^{-2\hat{\mathbf{\Delta}}(\hat{\mathbf{R}})^2\tau_p^2}\cdot\hat{\boldsymbol{\mu}}^2$, where τ_p and $E_{p,0}$ denote the probe pulse FWHM and maximum field amplitude. $\hat{\boldsymbol{\mu}}_p$ is the transition dipole moment. The probe pulse central frequency, ω_p, determines the difference potential, $\hat{\mathbf{\Delta}}(\hat{\mathbf{R}}) = V_e(\hat{\mathbf{R}}) - V_g(\hat{\mathbf{R}}) - \hbar\omega_p$. The window operators are sketched in Fig. 1 assuming identical pump and probe pulse frequencies and FWHM.

The dynamics of the 'hole' is illustrated in Fig. 1 for a weak pump pulse ($\mathcal{E}_P = 1.5\,\mathrm{nJ}$): The blue curve depicts the wave function just after the pump pulse, at $t = 24$ ps (taking $t = 0$ to be the time of the pump pulse maximum). A probe measurement at that time will find

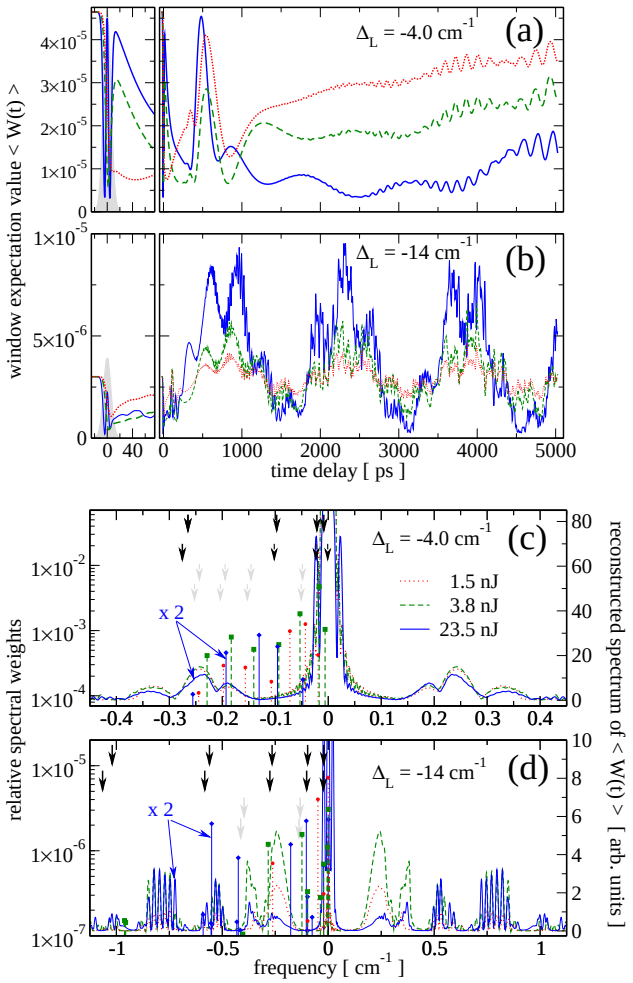

FIG. 3: (Color online) Probing the two-body correlation dynamics: time-dependent probe signal as a function of pump-probe delay (a+b) and probe spectrum (c+d) for pump pulse detunings $\Delta_L = -4.0\,\mathrm{cm}^{-1}$ (a,c) and $\Delta_L = -14\,\mathrm{cm}^{-1}$ (b,d) and three pump pulse energies. The black arrows indicate the position of the binding energies of the triplet (upper row) and singlet (lower row) levels, the grey arrows of half-multiples of the binding energies. The spectra for 23.5 nJ (blue solid lines) are scaled down by a factor of two.

no amplitude within the probe window. Due to the attractive ground state potential, the hole moves toward shorter distances, cf. the brown wave function Fig. 1 at $t = 126\,\mathrm{ps}$. This brings amplitude initially at larger R into the probe window. Eventually the motion of the 'hole' will be reflected at the repulsive barrier of the potential. The bound part of the wave packet will remain at short distance and oscillate, while the scattering part will pass through the probe window once not to return. This behavior is reflected in the transient probe absorption, i.e. the time-dependent window expectation value (red dotted curve in Fig. 3 a): The depletion of the signal due to the pump pulse, referred to as 'bleach' in traditional pump-probe spectroscopy, is followed by a recovery that peaks at 550 ps. At later times oscillations due to partial recurrence are observed but a full recovery does not occur. For larger detuning, Fig. 3b, a faster recovery of the bleach is observed at $t = 110\,\mathrm{ps}$. Obviously, the time to move from $R \sim 48\,\mathrm{a_0}$ to the repulsive barrier and back is shorter than that for $R \sim 76\,\mathrm{a_0}$.

Pump-probe spectroscopy can be used to probe the nodal structure of the initial pair wave function. The initial value of the window expectation value corresponds to probe absorption without a preceeding pump. The time-dependent signal can reach values above or below the initial one depending on the nodal structure of the initial pair wave function at the position R_L where the hole was created. At $\Delta_L = -4.0\,\mathrm{cm}^{-1}$ and $R_L \sim 76\,\mathrm{a_0}$, the Condon radius coincides with a maximum of the pair wave function. This implies maximum signal for probe absorption without pump. The slow dynamics of the delocalized hole wave packet is then unlikely to focus the amplitude in the probe window above its initial value. At $\Delta_L = -14.0\,\mathrm{cm}^{-1}$ and $R_L \sim 48\,\mathrm{a_0}$, the Condon radius is inbetween a node and a maximum, and amplitude initially at the nearby maximum moving inward can easily exceed the initial amplitude around the Condon radius.

The spectral decomposition of the 'hole' wave packet's bound part is unraveled by analyzing the oscillations in the transient probe absorption at long times. For large detuning the wave packet is made up of more strongly bound vibrational levels, cf. Fig. 2. Faster frequencies therefore characterize the oscillations in $\langle \hat{\mathbf{W}} \rangle(t)$, cf. Fig. 3 a and b. The spectra of these signals are obtained by filter-diagonalization [11], a method allowing to accurately extract frequencies from just a few oscillation periods; they are shown in Fig. 3 c and d. The vibrational periods of the bound ground state levels are recovered. Fig. 3 also confirms the observation from Fig. 2 that Rabi cycling during the pump pulse leads to a larger bound part in the 'hole', see the increase of spectral weights with pump pulse energy. While the projections of Fig. 2 would be difficult to access experimentally, wave packet spectral analysis via probe absorption is fairly straightforward.

Pure state vs thermally averaged dynamics Pump probe spectroscopy of the pair correlations can be applied to a quantum degenerate as well as a thermal ultracold gas. For the timescales and conditions considered here, quantum degeneracy implies that the gas is initially in a pure state while the thermal gas corresponds to an incoherent ensemble. Fig. 4 compares the transient probe absorption for the two cases. Thermal averaging introduces two effects – the finite width in scattering energies which is too small to be resolved on a nanosecond timescale, and the contribution of higher partial waves. The latter becomes particularly prominent in the presence of shape resonances. In order to highlight the role of shape resonances, Fig. 4 compares calculations including both singlet and triplet channels (a) to those for the

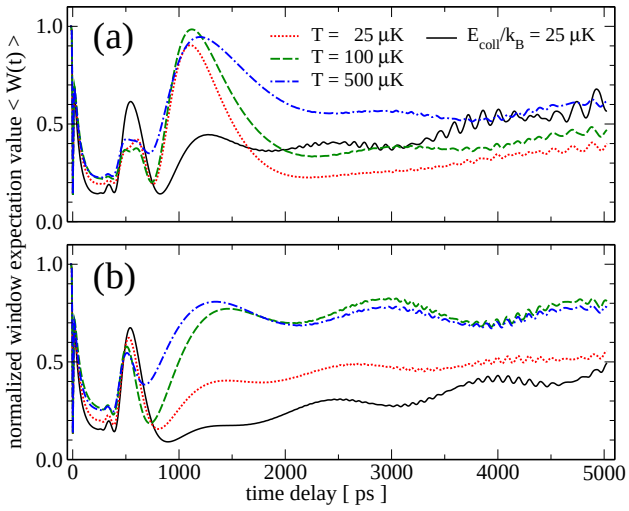

FIG. 4: (Color online) Pure state dynamics (black solid lines) vs those of a thermal ensemble (colored broken lines). For better comparability, the signal has been normalized with respect to the probe absorption without pump, ignoring scaling effects due to higher phase space density. (a) Singlet and triplet channels: The thermal dynamics are dominated by a singlet shape resonance while the pure dynamics shows features of both singlet and triplet dynamics. (b) Triplet channel only: The thermal and pure state dynamics are similar with the recovery of the bleach smeared out at higher temperatures. ($\Delta_{\rm L} = -4.0\,{\rm cm}^{-1}$, $\mathcal{E}_P = 3.8\,{\rm nJ}$)

triplet component only (b). Shape resonances are observed for $J = 2$ roughly at $160\,\mu$K and for $J = 6$ at about $430\,\mu$K in the singlet, and for $J = 2$ at $290\,\mu$K in the triplet channel. In Fig. 4 a and b, the recovery of the bleach at 550 ps is markedly smeared out but still visible in the thermally averaged calculations. At later times, a second peak is observed in Fig. 4 a at 1100 ps that corresponds to the singlet recovery of the bleach. In the thermal averages, the weight of the singlet contribution is significantly larger due to the shape resonance than in the pure state s-wave calculation. Since the Condon radius for the singlet channel is at larger distances than for the triplet channel, cf. Fig. 1, the singlet wave packet returns later to the probe window. This observation opens up the perspective of analysing pair wave functions in coupled channels scattering near a resonance where tuning an external field through the resonance will modify the respective weight of the channels. We emphasize that this novel pair correlation spectroscopy is possible even in the presence of e.g. three-body losses as long as the decay occurs on a timescale larger than a few nanoseconds.

Conclusions We have shown that pump-probe spectroscopy, a well established tool in chemical physics, can be utilized for the study of pair correlations in the quantum many-body system represented by an ultracold gas. Existing experimental setups [2, 3] need to be only slightly modified to implement our proposal. In particular, transform-limited pulses of about $1\,{\rm cm}^{-1}$ bandwidth are required for detection of the probe absorption via molecular ions. If one is able to provide for pump-probe delays of a few nanoseconds, spectral features on a scale of less than $1\,{\rm cm}^{-1}$ can be resolved. Pump-probe spectroscopy of the pair correlation dynamics can be combined with static external field control of the initial pair density. Specifically, tuning a magnetic field close to a Feshbach resonance may enhance the pair density at short and intermediate distances [12]. The resulting coupled channels pair wave function can be mapped out by spectral analysis of the pump probe signals. Future work will consider shaping the pump and probe pulses. For example, chirping the pump pulse changes the shape of the hole, while chirping the probe pulse allows for measuring the momentum of the hole. Once picosecond pulse shaping becomes available, the full power of coherent control can be employed to study pair correlation dynamics.

Acknowledgements We are grateful to F. Masnou-Seeuws and P. Naidon for many fruitful discussions and to the Deutsche Forschungsgemeinschaft for financial support.

* Electronic address: ckoch@physik.fu-berlin.de

[1] C. J. Pethick and H. Smith, *Bose-Einstein Condensation in Dilulte Gases* (Cambridge Univ. Press, 2002). A. J. Leggett, Rev. Mod. Phys. **73**, 307 (2001).
[2] W. Salzmann et al., Phys. Rev. Lett. **100**, 233003 (2008).
[3] D. J. McCabe et al., arXiv:0904.0244 (2009).
[4] T. Köhler and K. Burnett, Phys. Rev. A **65**, 033601 (2002). T. Köhler, T. Gasenzer, and K. Burnett, Phys. Rev. A **67**, 013601 (2003).
[5] P. Naidon and F. Masnou-Seeuws, Phys. Rev. A **68**, 033612 (2003). P. Naidon and F. Masnou-Seeuws, Phys. Rev. A **73**, 043611 (2006).
[6] V. Kokoouline, O. Dulieu, R. Kosloff, and F. Masnou-Seeuws, J. Chem. Phys. **110**, 9865 (1999). K. Willner, O. Dulieu, and F. Masnou-Seeuws, J. Chem. Phys. **120**, 548 (2004). S. Kallush and R. Kosloff, Chem. Phys. Lett. **433**, 221 (2006).
[7] C. P. Koch et al., J. Phys. B **39**, S1017 (2006).
[8] C. P. Koch, R. Kosloff, and F. Masnou-Seeuws, Phys. Rev. A **73**, 043409 (2006). C. P. Koch, F. Masnou-Seeuws, and R. Kosloff, Phys. Rev. Lett. **94**, 193001 (2005).
[9] E. Luc-Koenig, F. Masnou-Seeuws,and R. Kosloff, Phys. Rev. A **76**, 053415 (2007).
[10] L. W. Ungar and J. A. Cina, Adv. Chem. Phys. **100**, 171 (1997). E. Gershgoren, J. Vala, S. Ruhman, and R. Kosloff, J. Phys. Chem. A **105**, 5081 (2001).
[11] V. A. Mandelshtam and H. S. Taylor, J. Chem. Phys. **107**, 6756 (1997). V. A. Mandelshtam and H. S. Taylor, J. Chem. Phys. **108**, 9970 (1998).
[12] P. Pellegrini, M. Gacesa, and R. Côté, Phys. Rev. Lett. **101**, 053201 (2008).